FRA

Frontogenesis Elevates the Maximum Chlorophyll *a* Concentration at the Subsurface Near the Kuroshio During Well-Stratified Seasons

POC-P-17965

Daiki Ito[1] · Taketoshi Kodama[1,*] · Yugo Shimizu[1] · Takashi Setou[1] · Kiyotaka Hidaka[1] · Daisuke Ambe[1] · Sayaka Sogawa[1]
(1: Fisheries Research and Education Agency, Japan; *: Now at the University of Tokyo)

Frontogenesis improves primary productivity

- Frontogenesis is the development of oceanic fronts due to background deformation flows.
- Frontogenesis is accompanied by vertical currents and induces nutrient supply to the surface layer (e.g., Mahadevan 2016).

Does frontogenesis support productivity in the Kuroshio region during well-stratified season?

- The Kuroshio region has high biological productivity despite being in the subtropics and is a good spawning and nursery ground for pelagic fish (e.g., Okazaki et al. 2019).
- Limited studies have examined the contribution of frontogenesis to the productivity based on *in-situ* observation.

→ We examined the impact of fronts and frontogenesis on the distribution of subsurface chlorophyll *a* maximum ($\mathrm{CHL_{SCM}}$).

I. Increase of $\mathrm{CHL_{SCM}}$ near the front

- Intensive survey by R/V *Soyo-maru* on 26 August 2019
- T and S by CTD, u and v by the shipboard ADCP
- Analysis of discrete water samples: Nitrate and CHL
- The western side of the meander crest of the Kuroshio was zonally traversed (Horizontal resolution: ~ 9 km)

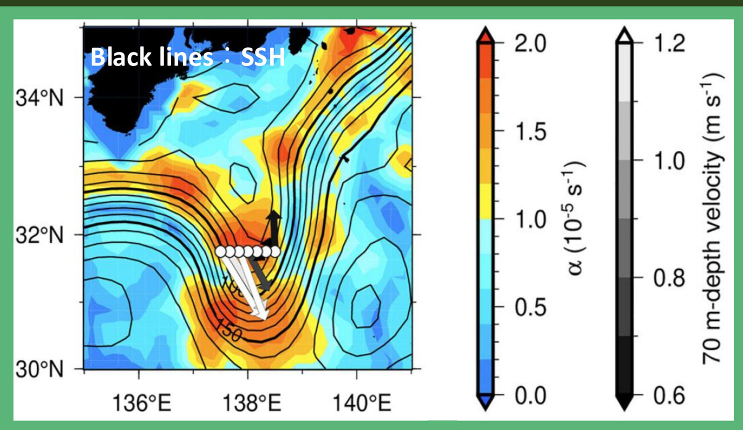

Indicator of horizontal deformation flow causing frontogenesis (lateral strain rate: α) was calculated by SSH as follows:

$$\alpha = \left[(U_x - V_y)^2 + (V_x + U_y)^2\right]^{1/2}$$

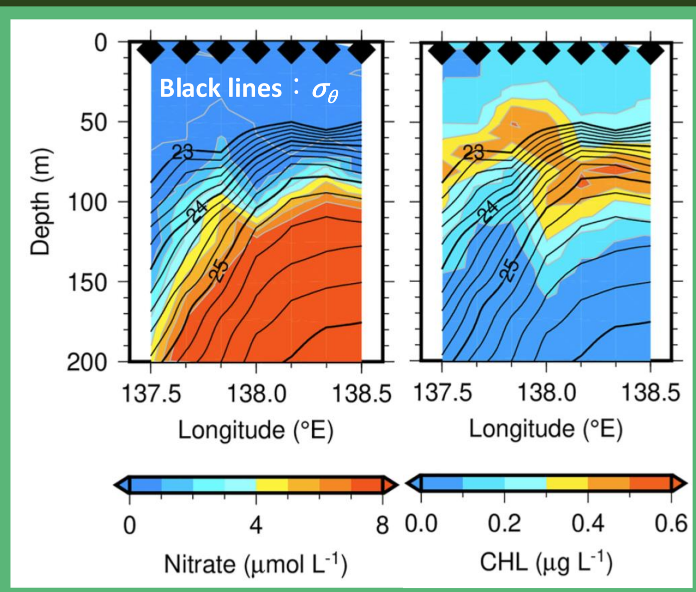

- Convergent flow in the cross-front direction
- Convex upward nitracline across isopycnals (~ 30 km)
- Particularly high $\mathrm{CHL_{SCM}}$ above the convex nitracline
- Diffusive upward nitrate flux: $F = \frac{\Gamma\varepsilon}{b_z} N_z$

  Assuming that $\Gamma = 0.2$ (Osborn 1980) and $\varepsilon = 10^{-8}\ \mathrm{m^2\,s^{-3}}$ (e.g., Kaneko et al. 2012), F was estimated as 10^{-6} mmol N $\mathrm{m^{-2}\,s^{-1}}$ (an order of magnitude larger than that outside the Kuroshio).

Schematic of nutrient supply and $\mathrm{CHL_{SCM}}$ increase caused by frontogenesis

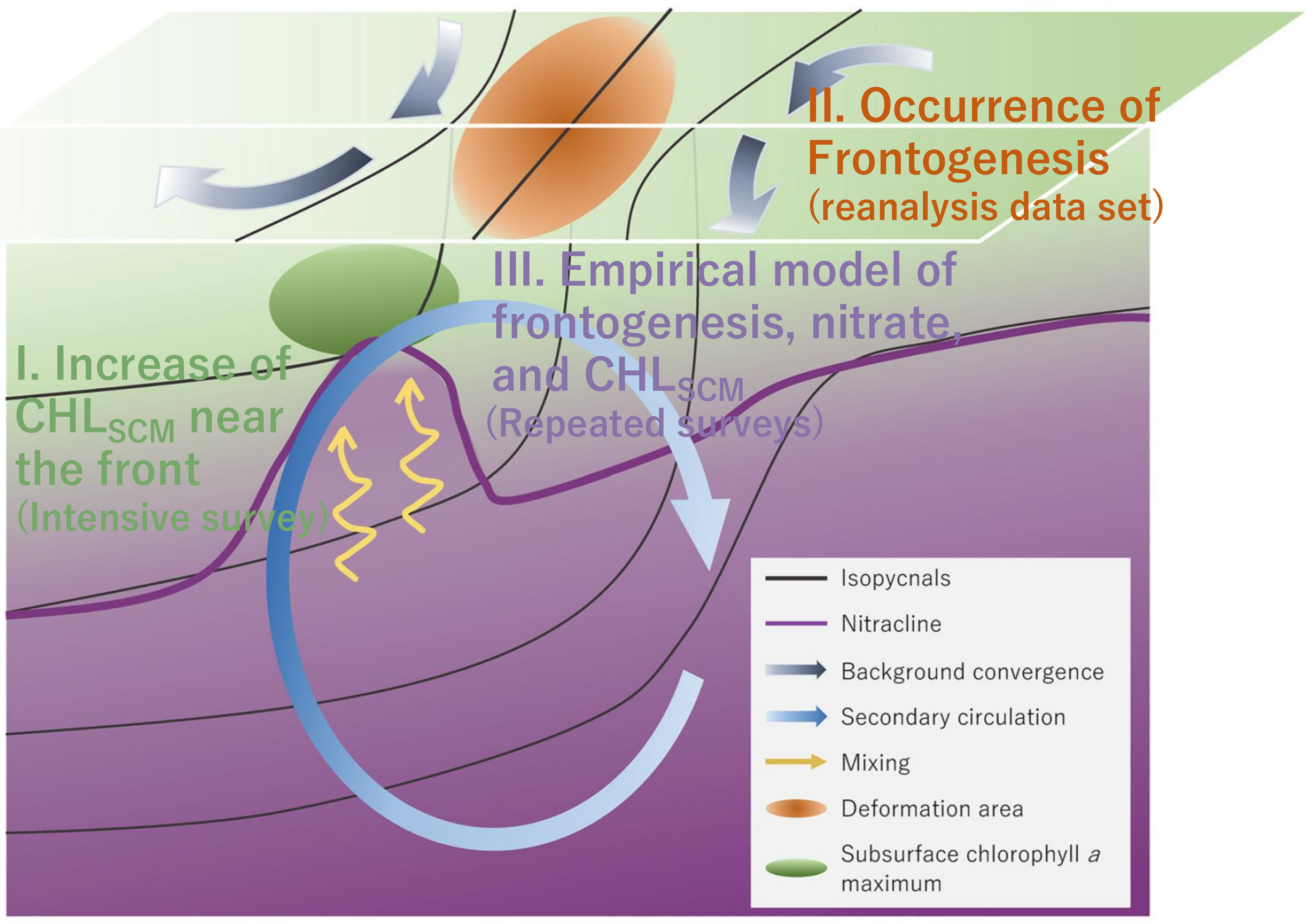

Key Points:

- Frontogenesis supplies nutrients and increases subsurface chlorophyll *a* concentration.
- Chlorophyll *a* concentration is positively correlated with the strength of fronts and frontogenesis.
- Subsurface chlorophyll *a* concentration is estimated using satellite-derived geostrophic velocity.

References

Mahadevan, A, 2016, Annu. Rev. Mar. Sci., 8(1), 171–184.
Okazaki, Y, et al., 2019, Geophysical Monograph 243, 245–256.
Osborn, TR, 1980, J. Phys. Oceanogr., 10, 83–89.
Kaneko, H, et al., 2012, Geophys. Res. Lett., 39, L15602.
Hirose, N, et al., 2019, Ocean Dyn. 69, 1333–1357.
Hoskins, BJ, 1982, Annu. Rev. Fluid Mech., 14, 131–151.

✓ The main results of this study have been published in JGR Oceans:
Ito, D, et al. 2023, J. Geophys. Res.: Oceans, 128(5), e2022JC018940.

II. Occurrence of Frontogenesis

- MOVE/MRI.COM-JPN reanalysis data set developed by Japan Meteorological Research Institute (Hirose et al. 2019) on 26 August 2019
- Resolution of 1/33° zonally and 1/50° meridionally (~2 km)
- To examine the frontogenesis, we calculated the time evolution of horizontal buoyancy gradient ($b = -g\rho/\rho_0$) (Hoskins 1982):

$$\frac{D}{Dt}\nabla b = \begin{bmatrix} -u_x b_x - v_x b_y \\ -u_y b_x - v_y b_y \end{bmatrix} \equiv \begin{bmatrix} Q_1 \\ Q_2 \end{bmatrix} = \mathbf{Q}$$

$$T_F = \frac{1}{2}\frac{D}{Dt}\|\nabla_h b\|^2$$

- Since the Kuroshio roughly flowed along meridians, we focused on the evolution of the zonal gradient ($b_x < 0$; Q_1).

- Stretching ($-u_x b_x < 0$) and tilting ($-v_x b_y > 0$) contributed to the increase of negative zonal buoyancy gradient ($Q_1 < 0$; i.e., frontogenesis).
- Even considering the meridional evolution (Q_2), frontogenesis occurred ($T_F > 0$).
- Frontogenesis largely detected by Lateral strain rate (α) calculated from SSH.

$-u_x b_x < 0$ $\quad$ $-v_x b_y > 0$

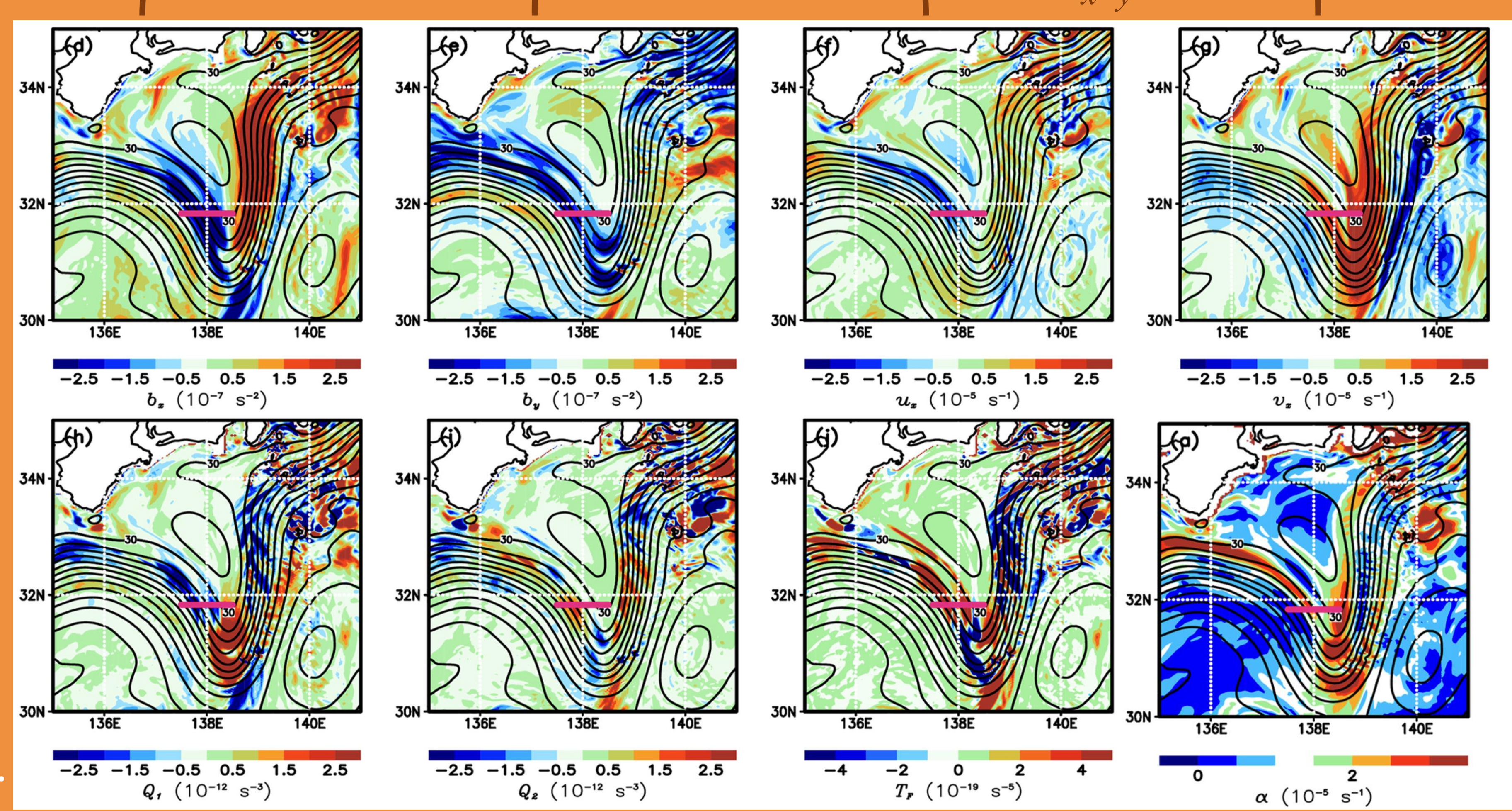

$Q_1 < 0$ $\quad$ $Q_2 > 0$ $\quad$ $T_F > 0$ $\quad$ α extracts Frontogenesis

III. Empirical model of frontogenesis, nitrate, and $\mathrm{CHL_{SCM}}$

- Summer and fall 10 cruise from 2014 to 2018 along 138°E (174 profiles)
- CTD, ADCP, and water samples (horizontal resolution: 50–100 km)
- Relationship between frontogenesis, nitrate, and $\mathrm{CHL_{SCM}}$ (Fig.)
- Generalized linear model (GLM) analysis was performed to verify the significant contribution of the variables to the $\mathrm{CHL_{SCM}}$ distribution

  ($b_{y\,\max}$: maximum value of absolute b_y, D_K: Distance from the Kuroshio axis, β: Intercept):

$$Z_{SCM} = glm(SSH + b_{y_{\max}} + \alpha + D_K + \beta)$$
$$Z_{SCM} = glm(Z_{N_1} + b_{y_{\max}} + \alpha + D_K + \beta)$$

- The shallower the depth of nitracline (Z_{N1}), the shallower Z_{SCM} and the larger is $\mathrm{CHL_{SCM}}$.
- The stronger the front (i.e., the larger $b_{y_{\max}}$) and the deformation (i.e., the larger α), the shallower Z_{N1} and Z_{SCM}, and the larger is $\mathrm{CHL_{SCM}}$.
- GLM analysis showed that the estimation accuracy of SCM distribution is improved by considering the dynamical features obtained from *in-situ* and satellite observations ($b_{y\max}$ and α); that is, Z_{SCM} becomes shallow and $\mathrm{CHL_{SCM}}$ becomes large when strong fronts exist, and frontogenesis occurs.

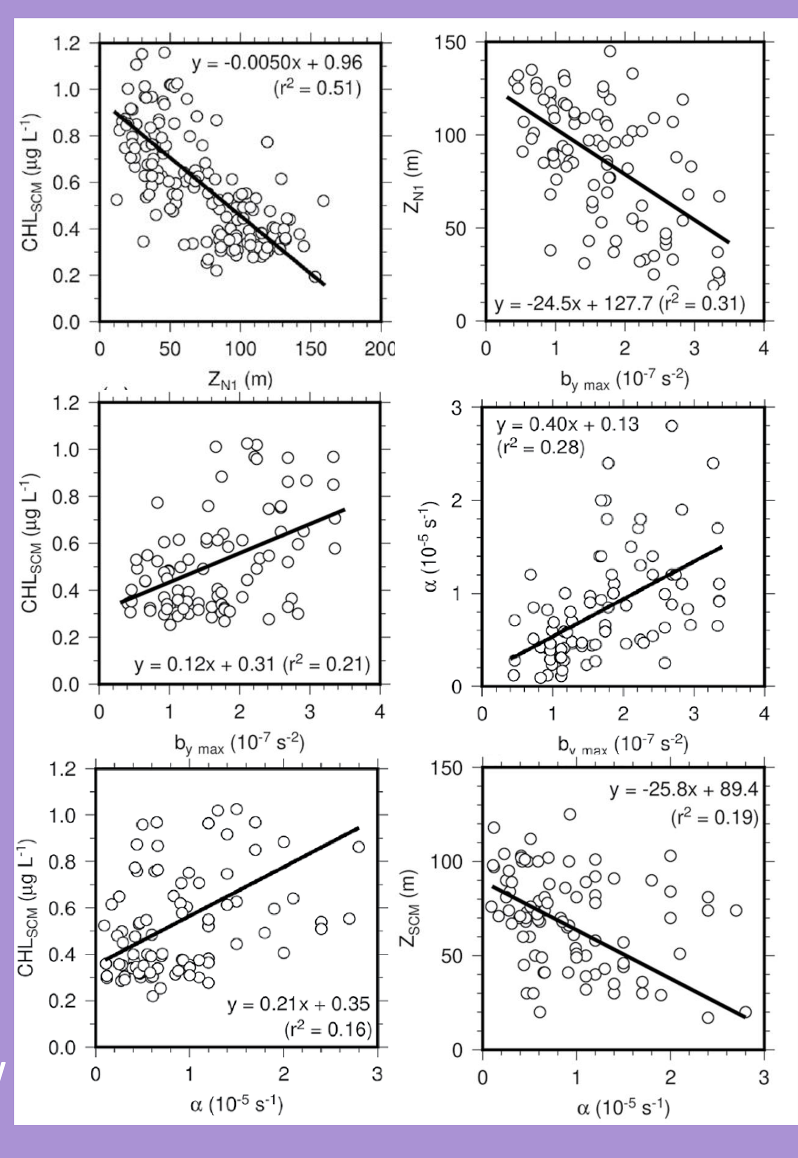

	Coefficient ± SE	t-value	p-value	ΔDE
(a) $Z_{SCM} \sim \mathrm{glm}(\mathrm{SSH} + b_{y\,\max} + \alpha + \beta)$				
β	21.67 ± 3.89	5.588	1.04×10^{-7}	
$b_{y\,\max} \times 10^5$	−7.42 ± 1.32	−5.62	8.90×10^{-8}	7%
$\alpha \times 10^6$	−3.79 ± 2.17	−1.75	0.0822	1%
SSH	0.399 ± 0.030	13.154	$<2 \times 10^{-16}$	39%
(b) $Z_{SCM} \sim \mathrm{glm}(Z_{N1} + b_{y\,\max} + \alpha + D_K + \beta)$				
β	25.8 ± 3.5	7.3	1.53×10^{-11}	
$b_{y\,\max} \times 10^5$	−2.46 ± 1.40	−1.755	0.0812	0%
$\alpha \times 10^6$	−4.38 ± 1.60	−2.749	0.0067	1%
D_K	1.85 ± 0.98	1.894	0.0601	1%
Z_{N1}	0.533 ± 0.042	12.576	$<2 \times 10^{-16}$	25%

- The explanatory variables were selected by Akaike information criterion (AIC).
- The fitting of the model were evaluated with deviance explained (DE = 100 × [1 − residual deviance/null deviance])
- The explained proportion was evaluated with the difference of DE from the least-AIC model and those in which the target explanatory variable was removed (ΔDE).
- DE of the models were> 62.8%